Parametric up conversion of the vacuum

Trevor W. Marshall
Department of Mathematics, University of Manchester, Manchester M13 9PL, U. K.
16, March, 1998

Abstract

The theory of parametric down conversion of the vacuum, based on a real zeropoint, or "vacuum" electromagnetic field, has been treated in earlier articles. The same theory predicts a hitherto unsuspected phenomenon — parametric up conversion of the vacuum. This article describes how the phenomenon may be demonstrated experimentally.
PACS numbers: 03.65 42.50

1 Introduction

Parametric down conversion (PDC) and parametric up conversion (PUC) have been known about since the earliest days of nonlinear optics[1, 2]. They occur when a light signal of frequency ω_1 is incident on a nonlinear crystal which is pumped by a laser of frequency ω_0. In PDC an idler of frequency $\omega_0 - \omega_1$ is emitted; in PUC this emitted frequency is $\omega_0 + \omega_1$.

In the case of PDC the name is rather anomalous, because the pumping converts ω_1 into $\omega_0 - \omega_1$, which can be either "down" or "up" relative to ω_1. The phenomenon has been given this name because, in the most studied case, the incident wave is a mode of the zeropoint or "vacuum" field, and we then see *two coupled modes* emerging from the crystal. Their frequencies are ω_1 and ω_2 with $\omega_1 + \omega_2 = \omega_0$. But the optical community has been reluctant to recognize the reality of the zeropoint field; in the early days of nonlinear optics it was sometimes called "fictitious"[3], but nowadays it is not afforded even this status. So, according to the current description, a "photon" of the laser with energy $\hbar\omega_0$ downconverts, spontaneously, into a pair of "photons" with energies $\hbar\omega_1$ and $\hbar\omega_2$. If we insist on the older, and in my view correct, description, this latter phenomenon should, properly, be called Parametric Down Conversion of the Vacuum (PDCV). What is occurring is the conversion of a zeropoint mode ω_1 into a detectable signal ω_2, and simultaneously the conversion of a zeropoint mode ω_2 into a signal ω_1.

The zeropoint description of PDCV has been investigated in a series of articles[4, 5, 6, 7], where we showed that it gives a consistent local realist explanation for all PDCV phenomena purporting to show photon entanglement. If we change over from the photon description to the wave description of light, all of these mysterious, allegedly "nonlocal" phenomena become local!

Now an obvious question to pose is "If the pump can convert a vacuum mode ω_1 into a detectable signal $\omega_0 - \omega_1$ (PDCV), why is it that nobody has reported

seeing the conversion of ω_1 into $\omega_0 + \omega_1$ (PUCV)?" My reply to this question is simply that nobody has looked for this phenomenon; if they look for it they will see it! All we need to know is where to look and, at least approximately, what intensity of signal to expect. We show how to do this in the following sections.

2 Position of the PUCV rainbow

The direction of a PDCV (or PUCV) signal is determined by the *phase matching condition*[1], which is that, at all points of the crystal and at all times, the phase of the pump coincides with the sum (or difference) of the phases of the two coupled zeropoint modes. In the case of PDCV this condition may be translated into "photon" language as Conservation of Four-Momentum, but no such translation exists for PUCV, which is possibly why nobody has looked for PUCV. We shall suppose the customary experimental setup, in which the pump is normally incident on one of the crystal faces. Then, if the refractive indices of the modes $(\omega_0, \omega_1, \omega_2)$ are (n_0, n_1, n_2), and the wave vectors of (ω_1, ω_2) make angles (θ_1, θ_2) with the pump, phase matching gives (upper signs are PDCV, and lower are PUCV)

$$\omega_2 = \omega_0 \mp \omega_1 \ , \tag{1}$$

$$\omega_2 \sqrt{n_2^2 - \sin^2\theta_2} = \omega_0 n_0 \mp \omega_1 \sqrt{n_1^2 - \sin^2\theta_1} \ , \tag{2}$$

$$\omega_2 \sin\theta_2 = \mp \omega_1 \sin\theta_1 \ . \tag{3}$$

Typically, solution of these matching conditions, for θ_1 and θ_2 in terms of ω_1, gives us PDCV and PUCV as depicted in Figure 1.

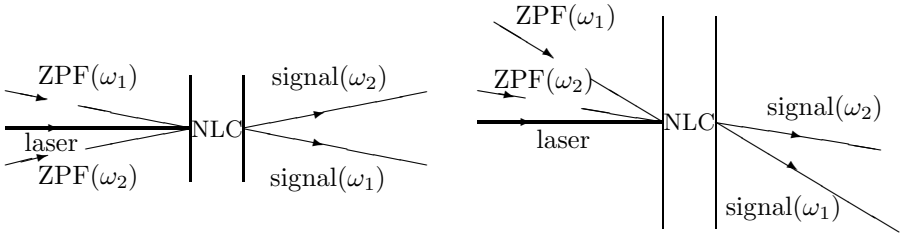

Figure 1: Typical PDCV (left) and PUCV(right) processes, as predicted by classical electrodynamics incorporating a real zeropoint field (ZPF). The latter modes have been denoted by interrupted lines, indicating that they are below the intensity threshold for detection. Note that the PDCV signal pair are on opposite sides of the pump, while the PUCV pair are both on the same side.

The wave vectors of the two outgoing modes in Figure 1 depend on the

refractive indices of the crystal. We present here an experimental design using the BBO crystal, which is already widely used[8] in PDC experiments, and for which the ordinary and extraordinary indices are[9] (wavelength in microns)

$$n^2_{\rm ord}(\lambda) = 2.7359 + \frac{.01878}{\lambda^2 - .01822} - .01354\lambda^2 \,, \quad (4)$$

$$n^2_{\rm ext}(\lambda, 90) = 2.3753 + \frac{.01224}{\lambda^2 - .01667} - .01516\lambda^2 \,, \quad (5)$$

$$\frac{1}{n^2_{\rm ext}(\lambda,\theta)} = \frac{\cos^2\theta}{n^2_{\rm ord}(\lambda)} + \frac{\sin^2\theta}{n^2_{\rm ext}(\lambda,90)} \,. \quad (6)$$

Suppose a BBO crystal is cut at $\theta = 90$ degrees, which means that its optic axis lies in one of its faces, and that a pump of wavelength 351nm is normally incident on that face and polarized in the ordinary direction, that is perpendicular to the optic axis. Then from the above matching conditions we may infer that, for most of the visible spectrum, that is for wavelengths $\lambda_1 > 481.07$nm, PUCV occurs in the form of a rainbow, that is each frequency is emitted in a definite direction. It should be emphasized that this direction is very different from that of the PDCV rainbow asssociated with ω_0, and in any case the latter is produced from a pump which is extraordinarily polarized.

The frequency-angle dependence of the lower-frequency mode is given in the following Table. For a given frequency the phase matching surface is a cone with its axis in the direction of the pump. Its cross section is an ellipse with the major axis in the equatorial plane, and the minor axis in the longitudinal plane, of the index ellipsoid. I give the semiangle of the cone in these two directions.

wavelength(nm)	equatorial semiangle(deg)	longitudinal semiangle(deg)	partner mode (*e*-polarized)
481.07	0	0	202.93
500	18.04	15.37	206.23
600	42.42	36.94	221.45
700	55.98	49.18	233.78
800	68.13	59.47	243.96

Table 1: PUCV with a normally incident pump at 351*o*. The lower-frequency signal, which is *o*-polarized, is in the three left-hand columns, while its undetectable *e*-polarized partner is in the right-hand column.

The title of *Up*-conversion refers in general to the fact that the *e*-polarized partner has a frequency higher than the pump, but, as we shall see in the next section, this mode actually has its intensity *reduced* below the zeropoint level, so that it cannot be directly detected. In the above example the whole of the *o*-polarized spectrum associated with PUCV was below the pump frequency, but

I emphasize that, in the zeropoint description, it is the "vacuum" rather than the pump which has its frequency converted. That there is no reason why the up-converted signal should necessarily have a lower frequency than the pump may be demonstrated by using a $702o$ instead of a $351o$ pump, as shown in Table 2.

wavelength(nm)	equatorial semiangle(deg)	longitudinal semiangle(deg)	partner mode (e-polarized)
256.79	0	0	188.01
270	28.04	16.99	195.00
300	45.57	28.69	210.18
400	65.08	44.23	254.81
500	73.16	51.69	292.01
600	79.67	56.93	323.50
679.5	89.33	60.47	345.28

Table 2: The same experimental setup as in Table 1, except that the pump wavelength is 702nm.

The most convenient part of the PUCV spectrum is probably those wavelengths which have exiting angles in the range from about 10-30 degrees. I give, in Table 3, the wavelength at the edge of the PUCV spectrum, where the exiting angle is zero. I note an interesting feature of this Table, namely that the partner mode near the edge of the PUCV spectrum is, in all cases, fairly close to, but above, the transparency limit of the crystal (189nm).

pump wavelength	edge of PUCV spectrum	partner mode (e-polarized)
351	481.07	202.93
400	419.35	204.72
500	338.02	202.00
600	290.02	195.51
702	256.79	188.01

Table 3: The edge of the PUCV spectrum as a function of the pump wavelength

The wavelengths used for an experimental observation of PUCV will be close to, but rather greater than, the edge wavelength. Obviously the most practical way to locate this relatively weak PUCV signal is to use a second laser suitably aligned. For example, with the $351o$ pump, a $206.23e$ laser in the equatorial plane, with an incidence angle of 7.34 degrees, will result in a relatively strong

PUC signal at 500nm and 18.37 degrees. Or, as an example where the up-converted mode has a frequency higher than the pump, consider a pump at 500nm. Then an aligning laser at 206.23nm, whose incidence angle is 12.71 degrees, will produce a signal at 351nm exiting at 18.37 degrees. The zeropoint theory predicts that the intensity of the PUC signal does not go to zero when this aligning laser is removed.

3 Intensity of the PUCV rainbow

We now calculate the intensity of the PUCV rainbow, using the crystal and pump geometry of the previous section. It is simplest to consider the signal emitted in the equatorial plane of the index ellipsoid, which we denote as the xy-plane; the pump's wave vector is $(\omega_0, 0, 0)$ and its polarization direction is $(0, 1, 0)$. So the signal has wave vector $(\omega_1 \cos\theta_1, \omega_1 \sin\theta_1, 0)$ and polarization direction $(-\sin\theta_1, \cos\theta_1, 0)$, while its partner mode has wave vector $(\omega_2 \cos\theta_2, \omega_2 \sin\theta_2, 0)$ and polarization direction $(0, 0, 1)$. We denote the magnitudes of the electric vectors of the three coupled modes as (E_0, E_1, E_2). Then the relevant crystal polarizations are

$$P_1 = \frac{n_1^2 - 1}{4\pi} E_1 + 2 d_{15} E_0 E_2 \cos\phi_1 \ , \tag{7}$$

$$P_2 = \frac{n_2^2 - 1}{4\pi} E_2 + 2 d_{31} E_0 E_1 \cos\phi_1 \ , \tag{8}$$

where ϕ_i gives the direction of a signal inside the crystal, that is

$$\sin\phi_i = \frac{\sin\theta_i}{n_i} \ , \tag{9}$$

and d_{15}, d_{31} are the appropriate second-order polarizabilities. Note that, with our choice of geometry, we have simply

$$n_0 = n_{\rm ord}(\omega_0) \ , \ n_1 = n_{\rm ord}(\omega_1) \ , \ n_2 = n_{\rm ext}(\omega_2, 90) \ . \tag{10}$$

We now make a linearizing approximation which is equivalent to neglecting the depletion of the pump inside the crystal, namely we put

$$E_0 = V \cos(\omega_0 t - k_0 x) \ , \ (k_0 = n_0 \omega_0) \ , \tag{11}$$

and treat V as constant. We also neglect dissipation within the crystal, and define

$$f_1 = 4\pi d_{15} V \cos\phi_1 \ , \ f_2 = 4\pi d_{31} V \cos\phi_1 \ . \tag{12}$$

Then the Maxwell equations coupling E_1 and E_2 are

$$(\Delta + n_1^2 \partial^2/\partial t^2) E_1 = -f_1 (\partial^2/\partial t^2) E_2 \cos(i\omega_0 t - i k_0 x) \ , \tag{13}$$

$$(\Delta + n_2^2 \partial^2/\partial t^2) E_2 = -f_2 (\partial^2/\partial t^2) E_1 \cos(i\omega_0 t - i k_0 x) \ . \tag{14}$$

Now we substitute

$$E_i(x,y,z) = \sqrt{\frac{\omega_i}{n_i}}[A_i(x)e^{i\omega_i' t - ik_i x - \omega_i \sin\theta_i y} + \text{c.c.}] \ , \tag{15}$$

where

$$\omega_1' \approx \omega_1 \quad , \quad \omega_2' = \omega_0 + \omega_1' \quad \text{and} \quad k_i = \sqrt{n_i^2\omega_i'^2 - \omega_i^2 \sin^2\theta_i} \ , \tag{16}$$

and put

$$g_i = \frac{f_i}{2\cos\phi_i}\sqrt{\frac{\omega_1\omega_2}{n_1 n_2}} \ , \tag{17}$$

and we make the slowly-varying-envelope approximation, that is we discard second derivatives of A_i. Then the coupling equations become

$$\frac{dA_1}{dx} = -ig_1 A_2 e^{i\Delta x} \ , \tag{18}$$

$$\frac{dA_2}{dx} = -ig_2 A_1 e^{-i\Delta x} \ , \tag{19}$$

where

$$\Delta = k_0 + k_1 - k_2 \ . \tag{20}$$

Note that, when $\omega_1' = \omega_1$, we have perfect phase matching, and then $\Delta = 0$. These equations are the generalization of Ref.[1], eq.(8.7-2); g_1 and g_2 differ because we are not putting $f_1 = f_2$, and also because the rays are not all collinear.

For a crystal of length l we may solve the above coupling equations and obtain the mode amplitudes at $x = l$ in terms of those at $x = 0$:

$$A_1(l)e^{-i\Delta x/2} = A_1(0)[\cos(bl) - i(\Delta l/2)\text{sinc}(bl)] - ig_1 l A_2(0)\text{sinc}(bl) \ , \tag{21}$$

$$A_2(l)e^{i\Delta x/2} = A_2(0)[\cos(bl) - i(\Delta l/2)\text{sinc}(bl)] - ig_2 l A_1(0)\text{sinc}(bl) \ , \tag{22}$$

where

$$\text{sinc}(x) = \frac{\sin x}{x} \quad \text{and} \quad b = \sqrt{(\Delta^2/4) + g_1 g_2} \ . \tag{23}$$

The corresponding relation between the x-components of the Poynting vectors, that is $\mathcal{P}_i = k_i A_i A_i^*/n_i$, is

$$\mathcal{P}_1(l) = [\cos^2(bl) + (\Delta^2 l^2/4)\text{sinc}^2(bl)]\mathcal{P}_1(0) + (k_1 n_2 g_1^2 l^2/k_2 n_1)\text{sinc}^2(bl)\mathcal{P}_2(0) \ , \tag{24}$$

$$\mathcal{P}_2(l) = [\cos^2(bl) + (\Delta^2 l^2/4)\text{sinc}^2(bl)]\mathcal{P}_2(0) + (k_2 n_1 g_2^2 l^2/k_1 n_2)\text{sinc}^2(bl)\mathcal{P}_1(0) \ . \tag{25}$$

In order to obtain the relation between the Poynting vectors of the incoming and outgoing waves, we need, in addition to the latter relations, the transmission coefficients at the crystal interfaces, which are[10]

$$\frac{\mathcal{P}_i(0)}{\mathcal{P}_i(\text{in})} = \frac{\mathcal{P}_i(\text{out})}{\mathcal{P}_i(l)} = 1 - r_i \ , \tag{26}$$

where

$$r_1 = \frac{\tan^2(\theta_1 - \phi_1)}{\tan^2(\theta_1 + \phi_1)} \ , \ r_2 = \frac{\sin^2(\theta_2 - \phi_2)}{\sin^2(\theta_2 + \phi_2)} \ . \tag{27}$$

Combining these two sets of relations, we obtain

$$\begin{aligned} \mathcal{P}_1^{(0)}(\text{out}) &= [1 - g_1 g_2 l^2 \text{sinc}^2(bl)](1 - r_1)^2(\hbar k_1/2n_1) \\ &\quad + g_1^2 l^2 \text{sinc}^2(bl)(1 - r_1)(1 - r_2)(\hbar k_1/2n_1) \ , \end{aligned} \tag{28}$$

$$\begin{aligned} \mathcal{P}_2^{(0)}(\text{out}) &= [1 - g_1 g_2 l^2 \text{sinc}^2(bl)](1 - r_2)^2(\hbar k_2/2n_2) \\ &\quad + g_2^2 l^2 \text{sinc}^2(bl)(1 - r_1)(1 - r_2)(\hbar k_2/2n_2) \ , \end{aligned} \tag{29}$$

where we have used the standard zeropoint spectrum, for which the Poynting vector of a mode $\mathbf{k}$ in free space is $(\hbar\mathbf{k}/2)$. The superscript (0) indicates that we have calculated the outgoing Poynting vectors after zero reflections. The contributions from a single reflection all originate in zeropoint modes coming, in Fig.2, from the right side of the crystal, and they give, to order $g_{1,2}^2$,

$$\begin{aligned} (2n_1/\hbar k_1)\mathcal{P}_1^{(1)}(\text{out}) &= r_1 + r_1(1 - r_1)^2[1 - g_1 g_2 l^2 \text{sinc}^2(bl)] \\ &\quad + r_2(1 - r_1)(1 - r_2) g_1^2 l^2 \text{sinc}^2(bl) \ . \end{aligned} \tag{30}$$

with a similar equation for $\mathcal{P}_2^{(1)}(\text{out})$. So zero and one reflections together give

$$\begin{aligned} (2n_1/\hbar k_1)\mathcal{P}_1^{(0+1)}(\text{out}) &= (1 - r_1^2 + r_1^3)[1 - g_1 g_2 l^2 \text{sinc}^2(bl)] \\ &\quad + [(1 - r_1 - r_2^2 + r_1 r_2^2) g_1^2 + r_1 g_1 g_2] \text{sinc}^2(bl) \ . \end{aligned} \tag{31}$$

The contributions from two reflections originate, as do those with zero reflections, in modes coming from the left. They should, strictly speaking, be superposed, but that would suppose what is probably an impossible accuracy in cutting the crystal, so we shall simply add their Poynting vector also, that is

$$\begin{aligned} (2n_1/\hbar k_1)\mathcal{P}_1^{(2)}(\text{out}) &= r_1^2(1 - r_1)^2[1 - g_1 g_2 l^2 \text{sinc}^2(bl)] \\ &\quad + (r_1^2 + r_2^2)(1 - r_1)(1 - r_2) g_1^2 \text{sinc}^2(bl) \ , \end{aligned} \tag{32}$$

giving

$$\begin{aligned} (2n_1/\hbar k_1)\mathcal{P}_1^{(0+1+2)}(\text{out}) &= (1 - r_1^3 + r_1^4)[1 - g_1 g_2 l^2 \text{sinc}^2(bl)] \\ + [\{1 - r_1 + r_1^2 - r_1^3 - r_2(1 - r_1)(r_1^2 + r_2^2)\} g_1^2 &+ (r_1 - r_1^2) g_1 g_2] \text{sinc}^2(bl) \ . \end{aligned} \tag{33}$$

The extension to all reflections is a straightforward piece of algebra[11]. We give the result

$$\begin{aligned} \mathcal{P}_1^{(0+1+2+\ldots)}(\text{out}) &= \frac{\hbar k_1}{2n_1}\left[1 + \frac{g_1(g_1 - g_2)l^2}{1 + r_1}\text{sinc}^2(bl)\right] \ , \\ \mathcal{P}_2^{(0+1+2+\ldots)}(\text{out}) &= \frac{\hbar k_2}{2n_2}\left[1 + \frac{g_2(g_2 - g_1)l^2}{1 + r_2}\text{sinc}^2(bl)\right] \ . \end{aligned} \tag{34}$$

The detection theory appropriate for a semiclassical theory like ours, which incorporates a real zeropoint field, is different from most semiclassical theories previously considered[12], because we suppose that detectors are activated only by signals whose intensity is above the zeropoint intensity. For details we refer to Ref.[7]. So the photocount rate $\mathcal{D}_i$, in the case of PUCV, will depend on the sign of $g_1 - g_2$. For the case $g_1 > g_2$ we will have

$$\mathcal{D}_2 = 0 \ , \ \mathcal{D}_1 = \mathcal{C}(\omega_1)\frac{\hbar k_1 \omega_1^2}{2n_1}\int_{\Delta\Omega_1}\int_{\Delta\omega_1}\frac{g_1(g_1-g_2)l^2}{1+r_1}\mathrm{sinc}^2(bl)d\omega_1' d\Omega_1 \ , \quad (35)$$

and, for $g_1 < g_2$,

$$\mathcal{D}_1 = 0 \ , \ \mathcal{D}_2 = \mathcal{C}(\omega_2)\frac{\hbar k_2 \omega_2^2}{2n_2}\int_{\Delta\Omega_2}\int_{\Delta\omega_2}\frac{g_2(g_2-g_1)l^2}{1+r_2}\mathrm{sinc}^2(bl)d\omega_2' d\Omega_2 \ , \quad (36)$$

where $\mathcal{C}(\omega_i)$ is a detector efficiency, $\Delta\Omega_i$ is the solid angle subtended by the detector at the crystal, and $\Delta\omega_i$ is the bandwidth which the detector accepts.

We have shown, therefore, that of the two "entangled" partners ω_1 and ω_2, only one is directly detectable; its partner is depleted below the zeropoint level and can not be detected. It seems plausible to suppose that the depleted partner is always ω_2, which is what happens when that mode is the pump. For this to be the case at the edge of the PUCV spectrum, displayed in Table 3 of the previous section, would require that $d_{15} \geq d_{31}$. We shall return to this question in a moment.

In the case of PDCV the whole calculation follows the same lines, and the result is the same except for certain changes of sign. We obtain

$$\begin{aligned}\mathcal{D}_{1D} &= \mathcal{C}(\omega_{1D})\,\frac{\hbar k_{1D}\omega_{1D}^2}{2n_{1D}}\int_{\Delta\Omega_{1D}}\int_{\Delta\omega_{1D}} \\ &\quad \frac{g_{1D}(g_{1D}+g_{2D})l^2}{1+r_{1D}}\mathrm{sinc}^2(b_D l)d\omega_{1D}' d\Omega_{1D} \ , \quad (37)\\ \mathcal{D}_{2D} &= \mathcal{C}(\omega_{2D})\,\frac{\hbar k_{2D}\omega_{2D}^2}{2n_{2D}}\int_{\Delta\Omega_{2D}}\int_{\Delta\omega_{2D}} \\ &\quad \frac{g_{2D}(g_{1D}+g_{2D})l^2}{1+r_{2D}}\mathrm{sinc}^2(b_D l)d\omega_{2D}' d\Omega_{2D} \ , \quad (38)\end{aligned}$$

where

$$b_D = \sqrt{(\Delta_D^2/4) - g_{1D}g_{2D}} \quad \text{and} \quad \Delta_D = k_0 - k_1 - k_2 \ . \quad (39)$$

These latter variables, in the PUCV case, are

$$b = \sqrt{(\Delta^2/4) + g_1 g_2} \quad \text{and} \quad \Delta = k_0 + k_1 - k_2 \ . \quad (40)$$

Since, in both cases, $g_1 g_2 l^2 << 1$, we may put simply

$$b = \Delta/2 \quad \text{and} \quad b_D = \Delta_D/2 \ . \quad (41)$$

Two detection procedures are commonly used; in one of them $\Delta\Omega$ is narrowly determined by a "pinhole" iris, while all frequencies are accepted by the detector; in the other the detector accepts only radiation which has passed through a narrow frequency filter $\Delta\omega$, but collects over a wide, effectively infinite, angular range. These procedures are completely equivalent, but the analysis used above is more easily continued in terms of the first one. An integration of the Δ-dependent part of the intensity, using the frequency dependence of Δ given by eq.(16) gives, approximately,

$$\int_0^\infty \mathrm{sinc}^2(\Delta l/2) d\omega_1' = \frac{2\pi}{l \mid n_1 \sec\phi_1 - n_2 \sec\phi_2 \mid} , \tag{42}$$

and in the PDCV case we obtain

$$\int_0^\infty \mathrm{sinc}^2(\Delta_D l/2) d\omega_1' = \frac{2\pi}{l \mid n_{1D} \sec\phi_{1D} - n_{2D} \sec\phi_{2D} \mid} . \tag{43}$$

Both of the latter approximations are good, provided we do not go too near the maximum, which occurs when the denominator on the right hand side is zero. There a more sophisticated approximation is required[3]; the integral is proportional to $l^{-1/2}$ instead of l^{-1} and dissipation can no longer be neglected.

I now want to compare the counting rate in a PUCV experiment, in which a pinhole is placed at an angle θ_1 corresponding to a signal whose frequency is near ω_1, with a PDCV experiment designed to detect a signal near ω_{1D}, whose pinhole is at θ_{1D}. Let us assume that both irises collect over the same solid angle. Then, substituting eqs.(17,42) in eq.(35), the counting rate for PUCV is

$$\mathcal{D}_1 = 16\pi^3 \hbar V^2 l \mathcal{C}(\omega_1) \Delta\Omega \, \frac{\omega_1^4(\omega_0+\omega_1)}{n_1 n_2} \, \frac{d_{15}(d_{15}\sec\phi_1 - d_{31}\sec\phi_2)}{\mid n_1\sec\phi_1 - n_2\sec\phi_2 \mid} \cdot$$
$$\cdot \, \frac{\cos^2\phi_1 \tan^2(\theta_1+\phi_1)}{\tan^2(\theta_1+\phi_1)+\tan^2(\theta_1-\phi_1)} . \tag{44}$$

The corresponding rate for ($e \to o + o$, equatorial) PDCV is

$$\mathcal{D}_{1D} = 16\pi^3 \hbar V^2 l \mathcal{C}(\omega_{1D}) \Delta\Omega \, \frac{\omega_{1D}^4(\omega_0-\omega_{1D})}{n_{1D} n_{2D}} \, \frac{d_{15D}^2(\sec\phi_{1D} + \sec\phi_{2D})}{\mid n_{1D}\sec\phi_{1D} - n_{2D}\sec\phi_{2D} \mid} \cdot$$
$$\cdot \, \frac{\cos^2(\phi_{1D}-\phi_{2D}) \tan^2(\theta_{1D}+\phi_{1D})}{\tan^2(\theta_{1D}+\phi_{1D})+\tan^2(\theta_{1D}-\phi_{1D})} . \tag{45}$$

Note that we should distinguish between d_{ij} and d_{ijD}, because these coupling constants depend on the participating mode frequencies. However, we do not yet have detailed information about such frequency dependence, so I shall now make the rather gross approximation that

$$d_{ijk} \text{ is independent of frequency and } d_{ijk} = d_{jik} , \tag{46}$$

so that d_{15}, d_{31} and d_{15D} are all equal. The second part of this approximation, known generally as the *Kleinman conjecture*[13], may be shown to be a consequence of the first. It is sometimes stated as a "theorem" (Ref.[2], page 780), despite some experimental evidence (Ref.[1], Table 8.1 and Ref.[2], Table 19.6-1) that d_{ijk} and d_{jik} can differ by up to 20 per cent. All that can safely be said is that the *approximate* frequency dependence of d_{ijk} incurs the *approximate* validity of the Kleinmann conjecture, which justifies its description[13] as "a powerful practical relationship". Note that this approximation gives $g_1 = g_2$ in the case of collinear PUCV, so that the intensity is then zero at the edge of the PUCV spectrum. Also, in the same spirit, we shall put $\mathcal{C}(\omega) =$ constant. Note that the quantity called "quantum efficiency" is $\hbar\omega\mathcal{C}(\omega)$.

The PDCV process which we take as a basis of comparison uses a $351e$ pump down-converting into two ordinarily polarized partners, one of which is $692o$ which corresponds to ω_{1D}. That brings us fairly close to the maximum counting rate for PDCV, which occurs for the symmetrical case $\lambda_1 = 702$nm. The ratio of $\mathcal{D}(\omega_1)$ to $\mathcal{D}(\omega_{1D})$ has been calculated, for various ω_1, using the approximations indicated in the previous paragraph, and the results are displayed in Table 4.

wavelength(nm)	$\mathcal{D}(\omega_1)/\mathcal{D}(\omega_{1D})$	θ_1(degrees)
482	0.003	4.07
484	0.011	7.20
486	0.025	9.33
488	0.059	11.04
490	0.254	12.50
492	0.221	13.81
494	0.094	14.99
496	0.065	16.08
498	0.052	17.09
500	0.045	18.04

Table 4: Ratio of PUCV to a standard PDCV counting rate as a function of wavelength.

We conclude that there is a peak in the intensity of the PUCV rainbow near 491nm, with a maximum counting rate around 30 per cent of the standard PDCV process. Of course, this PUCV maximum is nothing like as strong as the PDCV maximum at 702nm, but the above calculation indicates that it will nevertheless be easy to observe. Furthermore, the size of the maximum is extremely sensitive to a small departure from the approximation (46); if d_{31} is 5 per cent less than d_{15} it increases to somewhere between 100 and 150 per cent of the standard PDCV value.

4 Conclusion

We have shown, in the previous two sections, that PUCV, according to the theory of a real zeropoint field, must occur, and that it should not be too difficult to detect. Of course, observation of this phenomenon will be strong evidence in favour of a real ZPF.

We showed, in our earlier series of articles[4, 5, 6, 7], that the extremely problematic and nonlocal concept of *photon entanglement* between a coupled pair of PDCV signals receives a local and fully causal explanation in terms of a real ZPF. In the ZPF description, entangled photons are waves whose amplitudes are correlated below as well as above the level at which all detector thresholds are set. Now we find that, in PUCV, there is still a pair of entangled signals, but that one of them, that with its frequency above the pump frequency, is entirely below threshold, and therefore cannot be detected. Once PUCV has been experimentally demonstrated it will be a task for nonlinear opticians to devise ways and means of demonstrating this subzeropoint entanglement. One possible way to reveal the ghostly high-frequency partner would be to look for its mirror image emerging from the crystal in the backward direction. According to the analysis of the previous section this mode has an intensity above threshold, but the counting rate is reduced by a factor of r_2 relative to its forward low-frequency partner.

References

[1] A. Yariv, *Optical Electronics in Modern Communications*, (Oxford, New York, 1997), Chap.8.

[2] B. E. A. Saleh and M. C. Teich, *Fundamentals of Photonics*, (John Wiley, New York, 1991), Chap.19.

[3] D. A. Kleinman, *Phys. Rev.* **174**, 1027 (1968).

[4] A. Casado, T. W. Marshall, and E. Santos, *J. Opt. Soc. Am. B*, **14**, 494–502 (1997).

[5] A. Casado, A. Fernández Rueda, T .W. Marshall, R. Risco Delgado, and E. Santos, *Phys.Rev.A*, **55**, 3879–3890 (1997).

[6] A. Casado, A. Fernández Rueda, T. W. Marshall, R. Risco Delgado, and E. Santos, *Phys.Rev.A*, **56**, 2477-2480 (1997).

[7] A. Casado, T. W. Marshall and E. Santos, *J. Opt. Soc Am. B*, **15** (1998) (Article in proof). See also http://xxx.lanl.gov/abs/quant-ph/9711042.

[8] P. G. Kwiat, K. Mattle, H. Weinfurter, A. Zeilinger, A. V. Sergienko and Y. Shih, *Phys. Rev. Lett.*, **75**, 4337-4341 (1995).

[9] Ling Jiwu, *CASIX Technical Report*, P. O. Box 1103, Fuzhou, Fujian 350014, P. R. China.

[10] J. D. Jackson, *Classical Electrodynamics* (John Wiley, New York, 1962), pages 219-220.

[11] T. W. Marshall, *A local realist theory of parametric down conversion*, http://xxx.lanl.gov/abs/quant-ph/9711030.

[12] L. Mandel, *Progress in Optics*, **13**, 27 (1976).

[13] A. Yariv, *Quantum Electronics*, (John Wiley, New York, 1989), Chap.16.